

Three-Nucleon Force in the ^4He Scattering System

Hartmut M. Hofmann¹ and Gerald M. Hale²

¹ Institut für Theoretische Physik III, Universität Erlangen–Nürnberg, D–91058 Erlangen, Germany *hmh@theorie3.physik.uni-erlangen.de*

² Theoretical Division Los Alamos National Laboratory, Los Alamos N.M. 87544, USA *ghale@lanl.gov*

Summary. We report on a consistent, microscopic calculation of the bound and scattering states in the ^4He system employing modern realistic two-nucleon and three-nucleon potentials in the framework of the resonating group model (RGM). We present for comparison with these microscopic RGM calculations the results from a charge-independent, Coulomb-corrected R -matrix analysis of all types of data for reactions in the $A = 4$ system. Comparisons are made for selected examples of phase shifts and measurements from reactions sensitive to three-nucleon force effects.

Introduction

The ^4He atomic nucleus is one of the best studied few-body systems, both experimentally and theoretically, as summarized in the recent $A = 4$ compilation [1]. Besides the many textbook examples of gross structure, there are subtle points yielding large effects that are only qualitatively understood. Except for [2] none of the existing calculations aims at a complete understanding of the many features of ^4He , which is not surprising in view of the number of different phenomena studied so far [1]. With the recent compilation [1] and the comprehensive R -matrix analysis [3] of a large amount of scattering data below $E_x = 30$ MeV, a new, microscopic calculation for the ^4He system in this energy range using modern realistic two- and three-nucleon forces is most desirable.

It is well known that realistic nucleon-nucleon (NN) forces cannot reproduce the ^3H , ^3He , and ^4He binding energies. Three-nucleon interactions (TNIs) are added to give the necessary small corrections but they still fail to reproduce certain properties of the three nucleon system, most notably the A_y analyzing power in Nd scattering [4]. Yet the 30% deviation of A_y can be resolved by tiny changes in the Nd scattering phase shifts (on the order of 0.1 degrees [5, 6, 7]). Furthermore very many operators can contribute to a TNI and the lack of stringent conditions in the three-nucleon system on the structure of the TNI makes its application to other systems desirable. In [2] it was shown that although a realistic NN force can generally reproduce the

^4He system, there remain differences, most notably in the analyzing powers. Since the intensely studied ^4He system [1] is unfortunately very difficult to describe due to the many resonances and the ^4He bound state, the much simpler systems $p\text{-}^3\text{He}$ and $n\text{-}^3\text{H}$ where data exist in the energy range of interest were investigated in [8].

The essential findings of this work are that realistic NN interactions describe most of the phase shifts quite well but fail to reproduce the 3P_2 and 3P_0 phase shifts. The calculated splitting between these two channels is much too small, and neither the Urbana IX (UIX) [9] nor the TLA [10] three-nucleon force is able to improve the splitting significantly. In fact, there it is more important to include in the calculation negative parity states of the three-nucleon subsystem than one of these two TNIs. These findings suggest that new contributions to the NNN force acting on the P -waves should be considered, like an LS type TNI, as proposed in [11] for the $N-d$ analyzing powers, or the V_3^* operators proposed in [12]. Based on these findings we choose as NN force only the AV18 [13] and as TNI the Urbana IX [9] and in addition the V_3^* [12].

We organize the paper in the following way. The next section contains a brief discussion of the Resonating Group Model calculation together with the model spaces used. Then we compare R-matrix and RGM results of a few typical examples of scattering phase shifts for various model spaces and combinations of interactions. Finally we compare with data for examples sensitive to the TNIs.

RGM and model space

We use the Resonating Group Model [14, 15, 16] to compute the scattering in the ^4He system using the Kohn-Hulthén variational principle [17]. The main technical problem is the evaluation of the many-body matrix elements in coordinate space. The restriction to a Gaussian basis for the radial dependencies of the wave function allows for a fast and efficient calculation of the individual matrix elements [14, 16]. However, to use these techniques the potentials must also be given in terms of Gaussians. In this work we use suitably parametrized versions of the Argonne AV18 [13] NN potential and the Urbana IX [9] and the V_3^* [12]. The inclusion of an additional TNI requires almost two orders of magnitude more computing power than the realistic NN forces alone.

In the ^4He system we use a model space with six two-fragment channels, namely the $p\text{-}^3\text{H}$, the $n\text{-}^3\text{He}$, the $^2\text{H}\text{-}^2\text{H}$, the singlet deuteron and deuteron $\bar{d}\text{-}^2\text{H}$, the $\bar{d}\text{-}\bar{d}$, and the $(nn) - (pp)$ channels. The last three are an approximation to the three- and four-body breakup channels that cannot in practice be treated within the RGM. The ^4He is treated as four clusters in the framework of the RGM to allow for the required internal orbital angular momenta of ^3He , ^3H or ^2H .

For the scattering calculation we include the S , P and D wave contributions to the $J^\pi = 0^+, 1^+, 2^+, 0^-, 1^-$ and 2^- channels. From the R -matrix analysis these channels are known to give essentially the experimental data. (We discuss cases where this is not the case.) The full wave functions for these channels contain over 200 different spin and orbital angular momentum configurations, hence it is too complicated to be given in detail. The simplest wave functions we use for ${}^3\text{He}$ are those described in [8].

This small 29-dimensional model space yields -6.37 MeV binding energy, an *rms* radius of 1.78 fm and a D state probability of 7.7% for the ${}^3\text{He}$ using AV18. In order to avoid fake effects the relative thresholds in ${}^4\text{He}$ should be reproduced well, therefore we used also a 35-dimensional modelspace, called large, by allowing additional configurations with two orbital angular momenta on the two Jacoby coordinates yielding -6.69 MeV binding energy. This must be compared to -6.92 MeV known from Faddeev calculations [18]. For the deuteron we use the structure given in [2], yielding a binding energy of -1.921 MeV, which could be easily improved. But then the relative threshold energies deteriorate, see table 1. All the Gaussian width parameters were obtained by a non-linear optimization using a genetic algorithm [19] for the combination AV18 and UIX.

Once the fragment wave functions are fixed the scattering problem is solved with our RGM code relying on the Kohn-Hulthén variational principle [17]:

$$\delta(\langle\Psi_t|H - E|\Psi_t\rangle - \frac{1}{2}a_{ii}) = 0,$$

where a_{ij} denotes the reactance matrix.

The model space described above (consisting of four to ten physical scattering channels for each J^π) is by no means sufficient to find reasonable results. So-called distortion or pseudo-inelastic channels [16] have to be added to improve the description of the wave function within the interaction region. Accordingly, the distortion channels have no asymptotic part.

For practical purposes it is obvious to reuse some of the already calculated matrix elements as additional distortion channels. In that way we include all the positive parity states of the three-nucleon subsystems with $J_3^\pi \leq 5/2^+$ in our calculation. However, it was recently pointed out by A. Fonseca [20] that states having a negative parity J_3^- in the three-nucleon fragment increase the n - ${}^3\text{H}$ cross section noticeably. Therefore we also added the appropriate distortion channels in a similar complexity as in the J_3^+ case to our calculation, thereby roughly doubling the size of the model space. The 20 percent increase of the model space for the 3N bound states from 29 to 35 resulted in almost a factor of two in the computing time. The parameters of the V_3^* TNI were adjusted that the binding energy of triton and ${}^3\text{He}$ did change by less than 10 keV. Therefore we do not give the corresponding energies in table 1.

Table 1. Comparison of experimental and calculated total binding energies and relative thresholds (in MeV) for the various potential models used

potential	E_{bin}		E_{thres}	
	${}^3\text{H}$	${}^3\text{He}$	${}^3\text{He} - p$	$d - d$
av18	-7.068	-6.370	0.698	3.227
av18, large	-7.413	-6.588	0.725	3.572
av18 + UIX	-7.586	-6.875	0.710	3.745
av18 + UIX,large	-8.241	-7.493	0.748	4.400
exp.	-8.481	-7.718	0.763	4.033

Results

Since we are mainly interested in the effects of 3N-forces, we mention the bound state results only briefly. In the large model space AV18 plus UIX yields -27.81 MeV close to the experimental -28.296 MeV, to which the parameters of the UIX are fitted to. Although the parameters of the V_3^* TNI were chosen as to give only minute changes in the three-nucleon system, for ${}^4\text{He}$ it resulted in 650 keV additional binding.

The most detailed comparison between calculation and data is on the level of an energy dependent phase-shift analysis. This is given by the R-matrix analysis as described in [2] in detail. The lowest channel, triton-proton contains the intriguing first excited state of ${}^4\text{He}$, a 0^+ -resonance, sometimes considered a breathing mode, which is clearly seen in the 0^+ phase shift, see fig. 1, but does not show-up in the angular distributions, see fig. 3. Neglecting the Coulomb force this resonance is moved just below the p-triton threshold, i.e. it becomes a bound state, bound by less than 50 keV depending on the force and model space used. Therefore all approaches, which neglect the Coulomb force like [20] cannot aim at this energy region. In fig. 1 the R-matrix results are compared to the pure NN-calculations for various model spaces. For the small model space the calculation is slightly above the R-matrix data. Adding the negative parity distortion channels, we find a small increase due to the enlarged attraction. This effect is much smaller than the one found in triton-neutron scattering [20, 8]. Increasing the 3N-model space reduces the phase shifts considerably, due to the better ${}^4\text{He}$ binding and the additional thresholds shifted to higher energy, see table 1. In fig. 2 we find strong sensitivity to the additional TNI. This sensitivity in specific partial waves might help to unravel the operator structure of the TNI, especially as all the thresholds are unchanged from UIX to V_3^* .

For 58 and 120 degrees exist measured excitation functions for the p-triton differential cross section. For the forward angle the R-matrix analysis is on top of the data [21], the pure NN-calculation a bit below, with UIX almost on top of the data and with V_3^* a bit above. Since there are only minor differences, we do not show them. For the backward angle, however, see fig. 3, even the

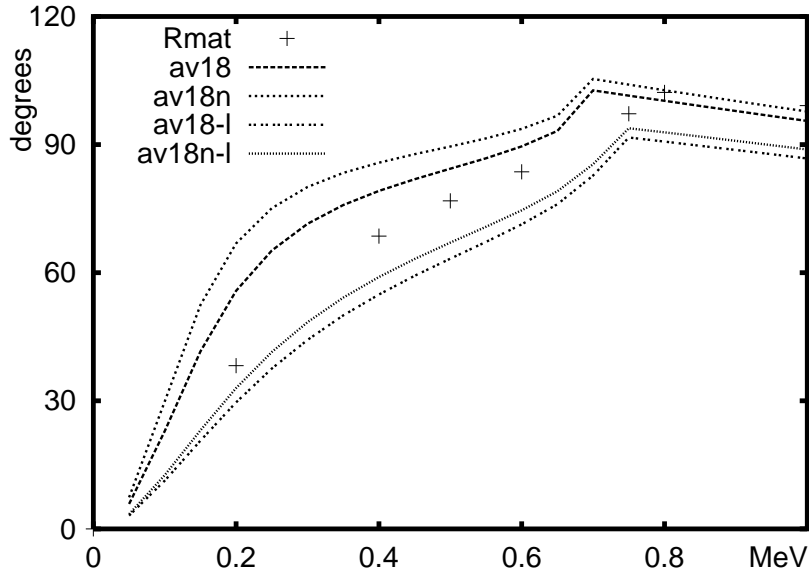


Fig. 1. Comparison of the 0^+ triton-proton phase shifts from the R-matrix analysis (crosses) and calculations employing AV18 in the small model space (av18), adding negative parity distortion channels (av18n), for the large model space (av18-l) and adding negative parity distortion channels (av18n-l)

R-matrix analysis cannot fully reproduce the data in the Coulomb-nuclear interference region. The data from [23] seem to be consistently above those from [21] and [22]. In the Coulomb-nuclear interference the sensitivity to TNI is very large, whereas around the (p,n) threshold data, R-matrix and microscopic calculations agree essentially. Since all the data are very old and not consistent a new measurement is urgently called for. Unfortunately due to radiation hazards of the triton this is not very likely.

A recent measurement of the real parts of the neutron- ${}^3\text{He}$ spin-dependent scattering lengths [24] $a_0 = 7.370(58)$ fm and $a_1 = 3.278(53)$ fm is therefore very important. The corresponding R-matrix results are $a_0 = 7.398$ fm and $a_1 = 3.257$ fm. Due to the strong coupling via the 0^+ resonance a_0 has a large imaginary part. Hence, the numerical extraction of this scattering length is not easy. Therefore we give only preliminary numbers in the following. For the large model space the microscopic calculations yield $a_0 = 7.402 \div 7.590$ fm and $a_1 = 3.289 \div 3.424$ fm, depending on the combination of forces. These results are close enough to be used for a further determination of the operator structure of the three-nucleon force.

Out of the many possible data we choose an example, which demonstrates the limitation of our total partial wave model space. The well studied deuteron-deuteron reactions allow a detailed comparison since together

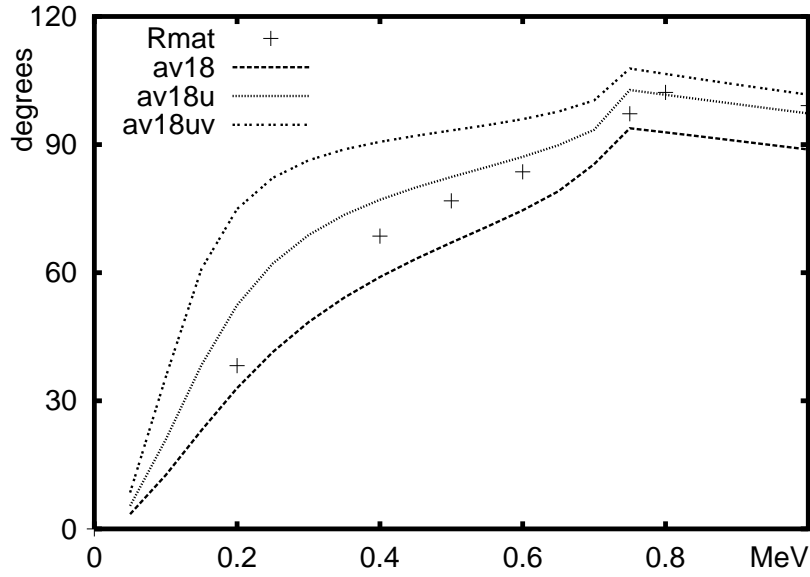


Fig. 2. As fig 1, but R-matrix results (crosses) are compared to the full NN-calculation (av18), adding UIX (av18u) and adding V_3^* (av18uv)

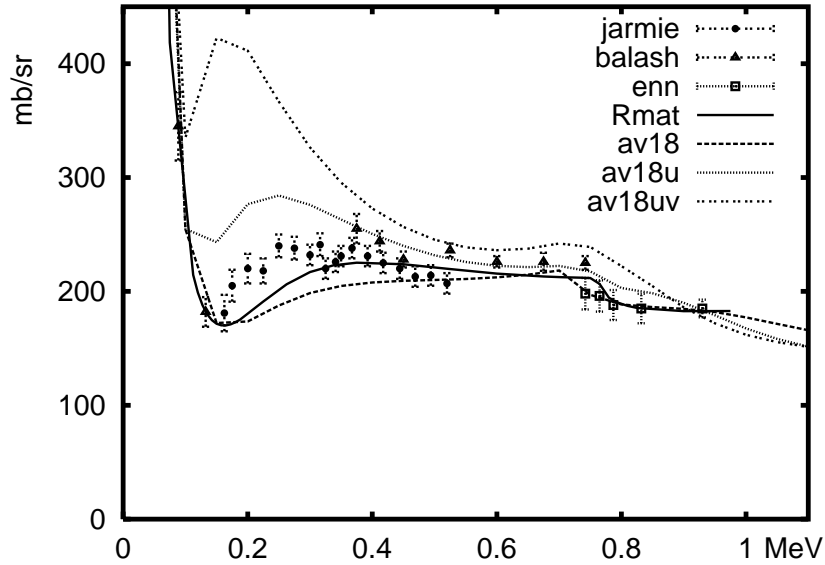


Fig. 3. Differential triton-proton cross section at 120 degrees as function of energy. The data are from Jarmie [21], Balashko [23], and Ennis [22]. The other lines are as in fig 2.

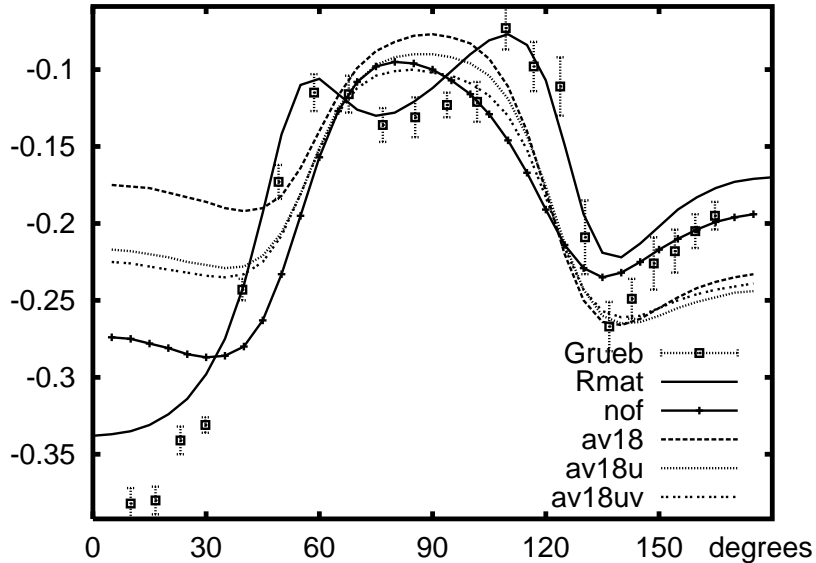


Fig. 4. Tensor analysing power T_{20} for the reaction ${}^2\text{H}(d,p){}^3\text{H}$ at 2.0 MeV center-of-mass energy. The data are from [25], the lines are as in fig 2 and additionally the R-matrix results without F-waves (nof).

with differential cross sections for many energies also analysing powers are available. The tensor analysing power T_{20} displays a pronounced angular distribution, see fig. 4. The full R-matrix analysis nicely reproduces the data, whereas all microscopic calculations fail at forward angles and show no sign of the double-hump structure. Omitting all F-wave S-matrix elements in the R-matrix analysis corresponding to the model space used for the RGM calculation yields an angular dependence quite similar to the microscopic results, see fig. 4. This demonstrates the need for $L_{rel} = 3$ partial waves in the RGM calculations.

Conclusion

We presented a complete microscopic calculation in the ${}^4\text{He}$ system employing modern realistic two- and three-nucleon forces. We demonstrated that in specific examples the inclusion of NNN-forces yields large effects in phase shifts, differential cross sections and analysing powers. Hence, the ${}^4\text{He}$ -system seems well suited for a detailed study of different NNN-forces, especially since a comprehensive R-matrix analysis exists, which reproduces the vast amount of data for various reactions very well, thus allowing for a comparison on the level of individual partial waves. Therefore a determination of the

operator structure of the NNN-force is within reach, provided the microscopic calculations are converged. To aim at this goal the internal triton and ^3He wave functions have to be improved, such that the binding energy is within say 50 keV of the experimental value. This can only be achieved by a major increase of the model space. For the deuteron the corresponding modification is trivial. To describe the deuteron-deuteron reactions, we have to allow also for F-waves on all relative coordinates. All these improvements are relative straightforward, but require about a factor 5 in the CPU-time compared to the needs of the work reported here.

Acknowledgments: The work of H.M.H is supported by the BMBF (contract 06ER926) and that of G.M.H. by the Department of Energy. The grant of computer time at the HLRB and the RRZE is gratefully acknowledged. We want to thank G. Wellein and G. Hager at the RRZE for their help.

References

1. Tilley, D.R., Weller, H.R., Hale, G.M. (1992): Energy levels of light nuclei $A = 4$. Nucl. Phys. **A541** 1–104
2. Hofmann, H.M., Hale, G.M. (1997): Microscopic calculation of the ^4He system. Nucl. Phys. **A613** 69–106
3. Hale, G.M., Dodder, D.C., and Witte, K. (unpublished)
4. Witala, H., Hüber, D., Glöckle, W. (1994): Analyzing power puzzle in low energy elastic Nd scattering: Phys. Rev. **C49** R14–R16
5. Knutson, L. D., Lamm, L. O., McAninch, J. E. (1993): Determination of the Phase Shifts for p–d Elastic Scattering at $E_p = 3$ MeV. Phys. Rev. Lett. **71** 3762–3765
6. Kievsky, A., Rosati, S., Tornow, W., Viviani, M. (1996): Critical comparison of experimental data and theoretical predictions for N-d scattering below the breakup threshold. Nucl. Phys. **A607** 402–424
7. Kievsky, A., Tornow, W. (1999): Proton-Deuteron Phase-Shift Analysis above the Deuteron Breakup Threshold. TUNL Progress Report - XXXVIII, Durham, USA
8. Pfitzinger, B., Hofmann, H. M., Hale, G. M. (2001): Elastic p– ^3He and n– ^3H scattering with two- and three-body forces. Phys. Rev. **C64** 044003–044008
9. Pudliner, B. S., Pandharipande, V. R., Carlson, J., Pieper, S. C., Wiringa, R. B. (1997): Quantum Monte Carlo calculations of nuclei with $A \leq 7$. Phys. Rev. **C56** 1720–1750
10. Hüber, D., Friar, J. L., Nogga, A., Witala, H., van Kolck, U. (1999): New Three-Nucleon-Force Terms in the Three-Nucleon System. nucl-th/9910034
11. Kievsky, A. (1999): Phenomenological spin-orbit three-body force. Phys. Rev. **C60** 034001–034008
12. Canton, L., Schadow, W. (2000): Why is the three-nucleon force so odd? Phys. Rev. **C62** 044005–044013
13. Wiringa, R. B., Stokes, V. G. J., Schiavilla, R. (1995): Accurate nucleon-nucleon potential with charge-independence breaking. Phys. Rev. **C51** 38–51

14. Hofmann, H. M. (1987): Resonating Group Calculations in Light Nuclear Systems. In: Ferreira, L. S., Fonseca, A. C., Streit, L. (ed) Proceedings of Models and Methods in Few-Body Physics, Lisboa, Portugal 1986. Springer Lecture Notes in Physics **273** 243–282
15. Wildermuth, K., Tang, Y. C. (1977): A Unified Theory of the Nucleus. Vieweg, Braunschweig
16. Tang, Y. C. (1981): Topics in Nuclear Physics. Lecture Notes in Physics **145** Springer, Heidelberg
17. Kohn, W. (1948): Variational methods in nuclear collision problems. Phys. Rev. **74** 1763–1772
18. Nogga, A., Kamada, H., Glöckle, W. (2000): Modern nuclear-force predictions for the α -particle. Phys. Rev. Lett **85** 944–947
19. Winkler, C., Hofmann, H. M. (1997): Determination of bound state wavefunctions by a genetic algorithm. Phys. Rev. **C55** 684–687
20. Fonseca, A. C. (1999): Contribution of Nucleon-Nucleon P Waves to nt - nt , dd - pt and dd - dd Scattering Observables. Phys. Rev. Lett. **83** 4021–4042
21. Jarmie, N., Allen, R. C. (1959): $T(p,p)T$ scattering near the $T(p,n)^3\text{He}$ threshold. Phys. Rev. **114** 176–178
22. Ennis, M. E., Hemmendinger, A. (1954): Small angle cross section for the scattering of protons by tritons. Phys. Rev. **95** 772–775
23. Balashko, Y. G., Barit, I. Y., Dulcova, L. S., Kurepin, A. B. (1964): Elastic scattering of protons by tritons at energies below the threshold of the (p,n) reaction JETP (Soviet Physics) **19** 1281–1283
24. Zimmer, O., Ehlers, G., Farago, B., Humblot, H., Ketter, W., Scherm, R. (2002): A precise measurement of the spin-dependent neutron scattering length of ^3He . EPJdirect **A1** 1–28
25. Grüebler, W., König, V., Risler, R., Schmelzbach, P.A., White, R.E., Marmier, P. (1972): Nucl. Phys. **A193** 149–154